

1
2
3
4
5
6
7
8
9
10
11
12
13
14
15
16
17
18
19
20
21
22
23
24
25
26
27
28
29

Meta-analytic connectivity modelling of deception-related brain regions

Sarah K. Meier^{1,*}, Kimberly L. Ray², Juliana C. Mastan^{1,¶}, Savannah R. Salvage^{1,¶}, Donald A. Robin^{1,3,4,*}

¹ Department of Communication Sciences and Disorders Research Laboratories, University of New Hampshire, Durham, New Hampshire, United States of America

² Department of Psychology, University of Texas, Austin, Texas, United States of America

³ Interdisciplinary Program in Neuroscience and Behavior, University of New Hampshire, Durham, New Hampshire, United States of America

⁴ Department of Biological Sciences, University of New Hampshire, Durham, New Hampshire, United States of America

* Corresponding authors

Emails: sarah.meier@unh.edu (SKM), don.robin@unh.edu (DAR)

¶These authors contributed equally to this work.

30 **Abstract**

31 Brain-based deception research began only two decades ago and has since included a
32 wide variety of contexts and response modalities for deception paradigms. Investigations of this
33 sort serve to better our neuroscientific and legal knowledge of the ways in which individuals
34 deceive others. To this end, we conducted activation likelihood estimation (ALE) and meta-
35 analytic connectivity modelling (MACM) using BrainMap software to examine 45 task-based
36 fMRI brain activation studies on deception. An activation likelihood estimation comparing
37 activations during deceptive versus honest behavior revealed 7 significant peak activation
38 clusters (bilateral insula, left superior frontal gyrus, bilateral supramarginal gyrus, and bilateral
39 medial frontal gyrus). Meta-analytic connectivity modelling revealed an interconnected network
40 amongst the 7 regions comprising both unidirectional and bidirectional connections. Together
41 with subsequent behavioral and paradigm decoding, these findings implicate the supramarginal
42 gyrus as a key component for the sociocognitive process of deception.

43 **Introduction**

44 The motivation for researching the complex behavior of deception exists not only to
45 identify mechanisms of sociocognitive functioning, but also to further efforts to detect instances
46 of suspect behavior. Deception is a critical aspect of criminology and forensic/legal decision-
47 making. Deception may be defined as “the act of causing someone to accept as true or valid what
48 is false or invalid” [1]. Deception occurs at various levels of society even becoming apparent in
49 current politics. Specifically, deception occurs in social settings and requires a willful decision
50 from the individual deceiving another [2]. Young, preschool age children are able to comprehend
51 the concept of lying [3], indicating the quotidian nature of deception established early on in

52 cognitive and behavioral development. Psychological assessment of psychopathy even considers
53 one's ability to lie, deceive, or manipulate [4]. The evolutionary and developmental bases of both
54 verbal and non-verbal deception have previously been reviewed [3]. Moreover, uncovering
55 neural substrates of deception has recently become an important area of research. Brain-based
56 deception research began in attempts to advance traditional polygraph testing [5]. The first report
57 of the neuroanatomical correlates of deception used functional magnetic resonance imaging
58 (fMRI) metrics [6].

59 In their pioneering publication, Spence et al. [6] had participants answer yes/no questions
60 while undergoing fMRI to investigate the hypothesis that inhibition of truthful responses would
61 be associated with greater ventral prefrontal cortex (PFC) activation. The researchers also
62 investigated if the generation of a lie would be associated with greater dorsolateral PFC
63 (DLPFC) activity. Results showed that lying was associated with increased activation in bilateral
64 ventrolateral PFC (VLPFC) and anterior cingulate cortex (ACC) in addition to medial premotor
65 and inferior parietal cortices.

66 Langleben et al. [7] utilized the guilty knowledge paradigm to test the hypothesis that
67 participants would activate inhibitory brain regions involved in executive control while
68 withholding a truthful response. Results demonstrated that lying was associated with greater
69 ACC and left parietal cortex activation, replicating Spence et al.'s initial findings [6]. A feigned
70 memory impairment task (where normal individuals pretend to have memory loss) was
71 conducted by Lee et al. [8] showing that malingering was associated with increased activation in
72 bilateral DLPFC, inferior parietal, middle temporal, posterior cingulate cortices, and bilateral
73 caudate nuclei. Further exploration of deception and the brain was conducted by Ganis et al. [9]
74 who investigated well-rehearsed versus spontaneous lies. Both types of lies were associated with

75 greater activation in bilateral anterior PFC and bilateral hippocampal gyri. The aforementioned
76 studies consistently demonstrated converging evidence across differing paradigms that deception
77 involves the prefrontal and anterior cingulate regions of the brain.

78 As noted, deception has been examined using a wide range of tasks. While there are
79 consistent findings across many studies, some variance exists related to the brain regions
80 involved in deception. It is likely that the neural underpinnings of deception vary based on the
81 act of deception recruiting areas functionally associated with decision making, risk taking,
82 cognitive control, theory of mind, and/or reward processing [10]. Most often reported is
83 activation of prefrontal regions (DLPFC, VLPFC or ventromedial PFC) and ACC, in addition to
84 the inferior frontal gyrus (IFG). Also reported in the literature are the anterior insula, precuneus,
85 inferior parietal lobule (IPL), medial frontal cortex, and regions of the temporal lobe.

86 Three prior meta-analyses have addressed the issue of variable activation reported during
87 deception. Christ et al. [11] used activation likelihood estimation (ALE) to quantitatively identify
88 regions consistently more active during deceptive responses than truthful responses. ALE pools
89 3-dimensional coordinates in stereotactic space from task-based brain activation studies. Results
90 identified deception-related activation in the bilateral insula, bilateral IFG, bilateral medial
91 frontal gyrus (MFG), bilateral IPL/supramarginal gyrus (SMG), right thalamus, right ACC, left
92 internal capsule, and left PFC. Further, they found that 10 of 13 peak deception-related regions
93 were associated with working memory, inhibitory control, or task switching, which are all
94 components of executive function.

95 Lisofsky et al. [12] extended the work of Christ et al. [11] by including “more
96 ecologically valid and interactive experimental paradigms” in their meta-analysis. Lisofsky et al.
97 based their meta-analysis on the idea that deception is both a sociocognitive and executive

98 process, pursuing Christ et al.'s [11] finding of deception-related IPL activation that was not
99 correlated with aspects of executive control. Lisofsky et al. [12] found bilateral activations in
100 ACC, IFG, and insula in addition to bilateral activity in IPL, and left MFG. This network was
101 “almost the same network” Christ et al. [11] reported in their work.

102 The most recent meta-analysis of deception and the brain focused on the distinction
103 between a deliberate attempt to deceive and a true false memory when not telling the truth [13].
104 Yu et al. [13] also used ALE to separately evaluate deceptive versus truthful responses and false
105 memories versus true memories. Analysis of deceptive versus truthful responses revealed 10
106 significant clusters primarily in bilateral frontoparietal regions including IFG, superior frontal
107 gyrus (SFG), MFG, insula, SMG, and caudate. The researchers stated that findings discussed in
108 both previous meta-analyses [11,12] were not sufficient to warrant fMRI-use in high stakes legal
109 contexts for detecting deception. They believe their work added the key factor of considering
110 why falsehoods arise (to deceive or not to deceive), not simply if they do.

111 In the current study, we use the ALE method of coordinate-based meta-analysis [14,15].
112 By pooling 3-dimensional coordinates, ALE analyzes voxel-wise, univariate effects across the
113 various experiments and generates a probability distribution that is centered at the respective
114 coordinates [16,17]. Building on this meta-analysis, we examine how deception-related brain
115 regions are functionally connected using meta-analytic connectivity modelling (MACM) [15,18-
116 20]. MACM uses regions from ALE to quantify covariance patterns (networks) via patterns of
117 activation reported across a wide range of paradigms [15,18,21]. To our knowledge, this is the
118 first meta-analysis to conduct connectivity analyses in an investigation of deception and the
119 brain. The use of functional connectivity in studies of deception may provide greater insight into

120 its neuropsychological mechanisms, provided that the majority of cognitive processes are
121 supported by various brain networks, rather than single brain regions.

122 The aims of this meta-analysis are as follows: first, to replicate previously reported brain
123 regions consistently activated during deception across the varying task paradigms; and second, to
124 determine a functionally connected brain network distinct to deceptive behavior versus honest
125 behavior. Our a priori hypotheses are: first, that we would observe activation in prefrontal and
126 memory-related regions of the brain across the various paradigms; and second, that we would
127 observe functional connections involving those regions within the resultant network.

128 **Methods**

129 **Literature search criteria and study selection**

130 Peer-reviewed articles published prior to August 26th, 2020 were selected through
131 searches on PubMed. The Preferred Reporting Items for Systematic Reviews and Meta-Analyses
132 (PRISMA) guidelines [22] were followed, and the selection process is detailed in Fig 1. The
133 initial search keywords used were: (deceptive OR deception OR dishonest) AND (fmri OR
134 magnetic resonance imaging). The following filters were applied to the initial search results on
135 the database: human subjects, adults (18+), and English language. Additional databases (Google
136 Scholar and PsycInfo) were searched via similar terms for articles not on PubMed. Each article
137 was subsequently reviewed (first by abstract, then by full-text) for relevance to the study and
138 inclusion of all following criteria: 1) published between 2005 and 2020, 2) carried out via task-
139 based functional magnetic resonance imaging, 3) at least five healthy (human) adult subjects, 4)
140 peak activations were reported (x , y , z coordinates provided in either MNI (Montreal
141 Neurological Institute) space or Talairach; coordinates reported in Talairach space were
142 converted to MNI using GingerALE (version 3.0.2.) [14,17,23], 5) a contrast was reported

143 representing locations of greater activation for deceptive responding as compared to being
 144 truthful, 6) contrasts were calculated using a commonly accepted level of significance in a whole
 145 brain analysis, and 7) information regarding the task and stimulus material used were reported.

146 Any relevant contrast related to deceptive versus honest behavior ($D > H$) in a relevant
 147 article was included to provide a complete analysis of reported contrasts for deceptive or honest
 148 behavior. For example, “Lie > Truth” and “Identity Concealment > Control” were both
 149 considered comparisons between deceptive behavior and honest behavior. Any article reporting
 150 the opposite contrast was included in the supplemental analysis of all contrasts (i.e. “Truth >
 151 Lie”). Table 1 details all contrasts included in the $D > H$ ALE and MACM. S1 Table details all
 152 contrasts of included articles, including both deceptive > honest and honest > deceptive
 153 contrasts.

154 **Table 1. Contrasts included in Deceptive > Honest ALE.**

155

#	Reference	N	Foci	Contrast Reported	Deception Task	Paradigm Class (besides "Deception")
1	Abe et al., 2014	25	10	Dishonest + Honest > Control	Decision-making (harmful or helpful)	Finger Tapping/Button Press
			4	(Dishonest/Harmful + Honest/Harmful) >		
			3	(Dishonest/Helpful + Honest/Helpful) >		
			3	(Dishonest/Harmful + Honest/Harmful) > Dishonest/Harmful > Honest/Harmful		
2	Abe & Greene, 2014	8	1	Dishonest: Opportunity Win > No-Opportunity Win	Monetary Incentive Delay/Incentive Prediction	
			3	Dishonest: Opportunity Loss > No-Opportunity Loss		
		7	1	Ambiguous & Dishonest: Opportunity Win > No-Opportunity Win		
			7	Ambiguous & Dishonest: Opportunity Loss > No-Opportunity Loss		
3	Baumgartner et al., 2009	26	1	Promise Stage: Dishonest > Honest, (Promise - No Promise)^Dishonest - (Promise - No Promise)^Honest	Modified Economic Trust Game	Finger Tapping/Button Press, Competition/Cooperation, Reward
			1	Anticipation Stage: Dishonest > Honest, (Promise - No Promise)^Dishonest - (Promise - No Promise)^Honest		
			1	Anticipation Stage: Dishonest > Honest, ((No Promise - Promise)^Dishonest - (No Promise - Promise)^Honest), $p < 0.0001$		
			1	Anticipation Stage: Dishonest > Honest, ((No Promise - Promise)^Dishonest - (No Promise - Promise)^Honest), $p < 0.0005$		
			2	Anticipation Stage: Dishonest > Honest, ((No Promise - Promise)^Dishonest - (No Promise - Promise)^Honest), $p < 0.005$		

			2	Decision Stage A: Dishonest > Honest, ((Promise - No Promise)^Dishonest - (Promise - No Promise)^Honest), p<0.001		Competition/Cooperation, Flashing Checkerboard, Reward
			2	Decision Stage A: Dishonest > Honest, ((Promise - No Promise)^Dishonest - (Promise - No Promise)^Honest), p<0.005		
			1	Decision Stage B: Dishonest > Honest, ((Promise - No Promise)^Dishonest - (Promise - No Promise)^Honest)		Finger Tapping/Button Press, Competition/Cooperation, Reward
4	Bereczkei et al., 2015	16	2	Unfair - Control, High Machiavellian > Low Machiavellian	Trust Game (in fair or unfair situations)	Competition/Cooperation, Finger Tapping/Button Press, Video Games
			7	Fair - Control, High Machiavellian > Low Machiavellian		
5	Bhatt et al., 2009	18	9	Unfamiliar: Lie > Truth	Recognition/"Line-up"	Finger Tapping/Button Press, Face Monitor/Discrimination
			4	Familiar: Lie > Truth		
			4	Familiar (Lie > Truth) > Unfamiliar (Lie > Truth)		
6	Browndyke et al., 2008	7	7	Malingered Recognition Misses > Normal Recognition Hits	Recognition Memory/Feigned Memory Impairment	
			5	Malingered Recognition False Alarm Errors > Normal Recognition Correct Rejections		
7	Cui et al., 2014	16	8	Murderer Group: Deceptive Probe Answer Judged Truthful > Truthful Irrelevant Answer Judged Truthful	Mock Murder/Modified Guilty Knowledge Test	Finger Tapping/Button Press
			12	Positive Judgement Following Probe: Murderer Group > Innocent Group		
8	Ding et al., 2012	12	7	Identity Concealment > Control	Recognition/Identity Concealment	Finger Tapping/Button Press
			9	Identity Faking > Control		
9	Farrow et al., 2015	20	5	Impression-Management > Control	"Balanced Inventory of Desirable Responding"	Finger Tapping/Button Press
			2	Self-Deception > Control		
			7	Faking Bad > Control		
			7	Impression-Management Main Effects		
			2	Self-Deception Main Effects		
			29	(Impression Management Faking Bad & Self Deception Faking Good[+1]) vs. (Impression Management Faking Good & Self Deception Faking Good[-1]) Main Effects		
			14	Faking Bad Main Effects		
10	Fullam et al., 2009	24	2	Lie - Truth	Lying (about performing tasks)	Deception only
11	Greene & Paxton, 2009	14	2	Dishonest (Opportunity Win > No-Opportunity Win)	Computerized Coin Flips/Moral Judgement	Reward, Finger Tapping/Button Press
			7	Dishonest (Opportunity Loss > No-Opportunity Loss)		
12	Harada T, 2009	18	23	Lie Judgement - Gender Judgment (masked with Lie Judgement)	Control Gender Judgement/Moral Judgement/Lie Judgement	Deception only
			7	Lie Judgement - Moral Judgement (masked with Lie Judgement)		
13	Hayashi et al., 2014	37	6	Harmful/ Dishonest > Harmful/ Honest	Harmful or Helpful Story-telling	Finger Tapping/Button Press, Reasoning/Problem Solving
			3	Helpful/ Dishonest > Helpful/ Honest		
14	Ito et al., 2011	32	9	Main effect of 'Lie' (Neutral/Lie+Negative/Lie) > (Neutral/Truth+Negative/Truth)	Remembering Neutral and Emotional Events	Finger Tapping/Button Press, Cued Explicit Recognition/Recall
			8	Neutral/Lie > Neutral/Truth		
			8	Negative/Lie > Negative/Truth		
			5	Conjunction Analysis: Neutral/Lie > Neutral/Truth + Negative/Lie > Negative/Truth		
15	Ito et al., 2012	16	6	Execution: (Certain/Lie + Uncertain/Lie) > (Certain/Truth + Uncertain/Truth)	Modified Recognition Memory	Finger Tapping/Button Press, Cued Explicit Recognition/Recall

16	Jiang et al., 2015	32	19	Lie > True	Strategy Devising	Finger Tapping/Button Press
17	Kireev et al., 2013	36	19	(Conjunction) Deceptive Claim > Catch + Honest Claim > Catch	"Cheat" Card Game	Finger Tapping/Button Press
			27	Deceptive Claim > Catch		
			21	Deception Claim > Honest Claim		
			6	rCBF: Deceptive Claim > Catch		
18	Kozel et al., 2005	30	18	Lie - Truth, Model Building Group	Mock Crime/"Ring-Watch Testing"	Deception only
		31	14	Lie - Truth, Model Testing Group		
19	Kozel et al., 2009	22	30	Mock-Crime: Lie > True	Mock Crime/"Ring-Watch Testing"	Finger Tapping/Button Press
		26	15	No-Crime: Lie > True		
20	Langleben et al., 2005	26	19	Lie > Repeat Distracter	Modified Guilty Knowledge Test	Deception only
			4	Lie > Truth		
21	Lee et al., 2009	10	8	Intentional Faked Responses > Truthful Accurate Responses	Recognition/Feigned Memory Impairment	Cued Explicit Recognition/Recall
			3	Intentional Faked Responses > Truthful Error Responses		
22	Lee et al., 2010	14	11	Lie > True	Lying (about valence of pictures)	Finger Tapping/Button Press, Affective Pictures
			17	Positive: Lie > True		
			4	Negative: Lie > True		
			4	Conjunction Analysis (Lie > True, Positive + Negative)		
23	Lee et al., 2013	13	2	Main Effect of Cue, Lie > Truth	Facial Recognition	Face Monitor/Discrimination, Finger Tapping/Button Press
24	Lelieveld et al., 2016	44	6	Justifiable Lies > Honest Reports	Evaluating Lies of Others	Finger Tapping/Button Press
			6	Unjustifiable Lies > Honest Reports		
25	Lissek et al., 2008	13	19	Deception > Cooperation	Theory of Mind Task	Theory of Mind, Competition/Cooperation, Affective Pictures
			13	Deception > Cooperation/Deception		
			15	Cooperation/Deception > Cooperation		
26	Liu et al., 2012	14	16	Falsification Card > BL	Conditional Proposition Testing	Finger Tapping/Button Press, Reason/Problem Solving
			9	Falsification > Non-Falsification		
27	Marchewka et al., 2012	29	13	Lie > Truth (General + Personal)	Gender Identity Inventory	Finger Tapping/Button Press
			13	Lie > Truth (General)		
			15	Lie > Truth (Personal)		
		14	16	Males: Lie > Truth		
		15	9	Females: Lie > Truth		
		14	11	Males: General Lie > General Truth		
		15	11	Females: General Lie > General Truth		
			13	Males: Personal Lie > Personal Truth		
			3	Females: Personal Lie > Personal Truth		
28	McPherson et al., 2012	15	8	Tones: Feigned > Correct	Feigned Hearing Loss	Finger Tapping/Button Press, Tone Monitor/Discrimination
			8	Tones: Feigned > Incorrect		
			6	Words: Feigned > Correct		Finger Tapping/Button Press
29	Mohamed et al., 2006	5	8	Words: Feigned > Incorrect (Lie, Known Lie + Lie, Subjective Lie) > Rest, Non-Guilty Subjects	Mock Shooting	Deception only
30	Nunez et al., 2005	20	8	False > True	True or False Response to Yes/No Questions	Deception only
			7	False, Autobiographical > True, Autobiographical		Episodic Recall
31	Ofen et al., 2017	18	7	Conjunction Analysis: Lie > True, Episodic and Belief	Lying (about personal experiences or beliefs)	Finger Tapping/Button Press
			6	Deception Main Effects: Belief-lie > Belief-true & Episodic-lie > Episodic-true		
			13	Preparation-Lie > Preparation-True		
			11	Negative Correlation between Preparation-lie > Preparation-true and Deception Index		
32	Peth et al., 2015	20	10	Guilty Action > Neutral	Concealed Information Test	Finger Tapping/Button Press

			1	Guilty Intention > Neutral		
33	Phan et al., 2005	14	11	Lie > Truth	Modified Guilty Knowledge Test	Deception only
			8	Lie > Recognition		
34	Pornpattananangkul et al., 2018	31	5	Opportunity > No-Opportunity (covariate: Overall Dishonesty)	Modified Coin-guessing Task	Finger Tapping/Button Press
			4	Opportunity-Self > No-Opportunity-Self (covariate: Opportunity-Self Dishonesty)		Finger Tapping/Button Press, Reward
			7	Opportunity-Donation > No-Opportunity-Donation (covariate: Opportunity-Donation Dishonesty)		Finger Tapping/Button Press
			4	Opportunity-Self > Opportunity-Donation (covariate: Self Serving Dishonesty)		Finger Tapping/Button Press, Reward
			7	Opportunity > No-Opportunity		
			2	Opportunity-Self > Opportunity-Donation		
			4	Opportunity-Donation > Opportunity-Self		
35	Shao et al., 2017	48	3	Dishonest (D) > Truthful (T); Cue Phase	Modified Directed Lie Paradigm	Finger Tapping/Button Press, Face Monitor/Discrimination
			23	1	Low (L) > High (H) Psychopathic Personality Inventory, Dishonest > Truthful; Cue Phase	
			48	10	Initial Session (T1) > Testing Session (T2), Dishonest > Truthful; Cue Phase	
			23	8	(L(T2(D>T)>T1(D>T)) > H(T2(D>T)>T1(D>T))); Cue Phase	
			48	5	Dishonest > Truthful; Face-Responding Phase	
			4	4	Initial Session (Dishonest > Truthful) > Testing Session (Dishonest > Truthful); Face-Responding Phase	
			23	3	L(T2(D>T) > T1(D>T)) > H(T2(D>T) > T1(D>T)); Face-Responding	
			2	2	Low (Familiar > Unfamiliar) > High (Familiar > Unfamiliar)	
36	Spence et al., 2008	17	7	Lie - Truth	Decision-making (whether or not to lie)	Deception only
			11	11	[(Lie - Truth) - (Defy - Comply)]	
37	D. Sun et al., 2015b	17	5	Main effect of Response Type (Lie > Truth)	Face Familiarity/Directed Lying	Face Monitor/Discrimination, Finger Tapping/Button Press
			1	1	Interaction Effect between Response Type and Face (Familiar (Lie - Truth) > Unfamiliar (Lie - Truth))	
38	D. Sun et al., 2015a	25	5	Dishonest > Honest (Positive Effect)	Economic Game	Finger Tapping/Button Press, Reward
			2	2	Dishonest > Honest (Negative Effect)	
39	D. Sun et al., 2016	25	6	Dishonest > Honest	Economic Game	Finger Tapping/Button Press, Reward
			1	1	Computer (Dishonest-Honest) > Human (Dishonest-Honest)	
40	P. Sun et al., 2017	21	4	Main Effects of Decision (Lying > Honest)	Adapted Dictator Game (after Ball-guess Game)	Finger Tapping/Button Press, Reward
			1	1	Interaction between Financial Position & Decision (Lying - Honest) Non-Deprived > (Lying - Honest) Deprived	
41	Vartanian et al., 2012	15	7	Lying > Truthful	Match/Mismatch Detection	Finger Tapping/Button Press, Reasoning/Problem Solving
			11	11	Matched: Lying > Truthful	
			5	5	Mismatched: Lying > Truthful	
42	Wu et al., 2011	20	8	Bad Lie > Bad Truth	Evaluating Cultural Aspects of Lying	Finger Tapping/Button Press, Reasoning/Problem Solving
43	Yin et al., 2016a	44	13	Spontaneous Lie in Incorrect Prediction, Spontaneous Truth in Incorrect Prediction, Spontaneous Truth in Correct Prediction > Fixation	Modified Sic Bo Gambling	Gambling, Finger Tapping/Button Press, Reward
44	Yin & Weber, 2016b	38	4	Main effect of means (Lies > Truth)	Modified Cheap Talk Sender/Receiver Game	Competition/Cooperation
45	Yin et al., 2019	37	3	Lying > Truth-Telling	Color Reporting Game	Deception only

156 The number of participants, number of reported foci, deception task used, and paradigm class are
157 listed for each reference/contrast.

158 BrainMap software was used to carry out both ALE and MACM. BrainMap [24] is a
159 database that archives published coordinate-based results in standard brain space from
160 neuroimaging experiments [25]. At the time of analysis, the BrainMap Functional Database
161 contained over 3,400 papers consisting of over 16,900 experiments with over 76,000 subjects
162 and 131,500 coordinate locations. The software used in the following analyses are briefly
163 described here: Scribe (version 3.3) [16,26,27] allows users to submit data and meta-data from
164 selected publications; Sleuth (version 3.0.4.) [16,26,27] allows users to search for and retrieve
165 coordinate data and meta-data from various publications archived in BrainMap; GingerALE
166 (version 3.0.2.) [14,17,23] allows users to carry out ALE-based meta-analyses.

167 **Fig 1. PRISMA Diagram.** This diagram depicts the inclusion criteria and study selection
168 process [22].

169 **Activation likelihood estimation**

170 ALE [14,15] was carried out using activation coordinates from the included studies
171 (Table 1) and BrainMap's GingerALE software (version 3.0.2.) [14,17,23]. The primary ALE
172 conducted and reported was based on deceptive versus honest ($D > H$) behavior. This $D > H$
173 ALE included 45 studies and 127 experiments with 977 foci from 2,836 subjects. Subsequent
174 ALE analyses are reported in Supplementary Material (see S2 Table; all contrasts: deceptive
175 versus honest, honest versus deceptive, etc.).

176 We followed standardized procedures for performing ALE using BrainMap's software as
177 reported in the GingerALE user manual (Research Imaging Institute, 2013,
178 <http://www.brainmap.org/ale/manual.pdf>). For ALE meta-analysis, a set of coordinates, in

179 addition to any experimental meta-data (identified as suitable for the specific research question),
180 are retrieved via Sleuth. These coordinates are input to GingerALE and smoothed with a
181 Gaussian distribution to accommodate the associated spatial uncertainty (using an estimation of
182 the intersubject and interstudy variability typically observed in neuroimaging studies) [25]. A
183 statistical parameter (the ALE value) is computed which estimates convergence across brain
184 images and measures the likelihood of activation at each voxel in the brain. Additionally, the
185 ALE algorithm calculates the above-change clustering between experiments (random-effects
186 analysis) rather than between foci (fixed-effects) [25]. The ALE value is generated for each
187 voxel and converted into p values for identification of areas with scores higher than empirically-
188 derived null distributions [14,16,17]. Consistency of voxel activation across varying studies can
189 be assessed due to the fact that ALE values increase with the number of studies reporting
190 activated peaks at a voxel or in close proximity [3]. The cluster-level inference (family-wise
191 error) and the uncorrected p -value used to threshold the ALE image were both set to 0.001
192 (5,000 permutations) in GingerALE.

193 **Meta-analytic connectivity modelling**

194 MACM investigates whole brain coactivation patterns corresponding to a region of
195 interest (ROI) across a range of tasks. In contrast to resting state functional connectivity
196 analyses, MACM provides a measure of functional connectivity during a range of task-
197 constrained states [28]. Functional connectivity networks can be extracted by functional
198 covariances, in this case during various task paradigms. These networks exhibit interconnected
199 sets of brain regions that interact to perform specific perceptual, motor, cognitive, and affective
200 functions [29]. We used the BrainMap database to search for studies including healthy subjects
201 that report normal mapping activations that exist within the boundaries of a 3-D spherical ROI,

202 regardless of the associated behavioral condition. Whole brain activation coordinates from these
203 selected studies are then assessed for convergence using the ALE method. MACM then yields a
204 map of significant coactivations that provides a task-free meta-analytic model of the region's
205 functional interactions throughout the rest of the brain [25]. This approach examines brain region
206 co-activity above chance within a given seed region across a large and diverse set of
207 neuroimaging experiments such as those dealing with deception [18,21]. MACM analyses
208 resulting in ALE maps have been validated with diffusion tensor imaging (DTI) and connectivity
209 atlases (CocoMac) [18] and have been demonstrated to be the meta-analytic equivalent of
210 resting-state functional connectivity maps [30,31].

211 Coordinates of the seven peak activation clusters were identified through $D > H$ ALE and
212 used as seeds for seven subsequent MACM analyses. Using Mango (Multi-image Analysis GUI)
213 [32], binary NIfTI images of 6 mm spherical radius ROIs were created as masks around each
214 peak coordinate. A standard MNI brain template (*Colin27_T1_seg_MNI.nii*) was used to
215 visualize the ROI masks. Separate searches for each identified peak ROI were performed using
216 Sleuth. The criteria for each search were: 1) Activations: Activations only, 2) Context: Normal
217 Mapping, 3) Subject Diagnosis: Normals, and 4) the corresponding 6 mm spherical ROI in MNI
218 space. Studies matching this query were downloaded to Sleuth's workspace. (See S3 Table for
219 specific functional workspaces for each node.) Coordinates from downloaded experiments
220 matching the criteria were analyzed using GingerALE at minimum volume of 250 mm³ and a p -
221 value < 0.01 .

222 **Network modelling**

223 Network modelling from MACM analyses was carried out using the approach first
224 outlined in Kotkowski et al. [20]. To summarize this procedure, Mango was used to visualize the

225 uncorrected MACM overlay for each seed coordinate on an MNI template
226 (*Colin27_T1_seg_MNI.nii*). The uncorrected estimate of meta-analytic connectivity between
227 each seed region and all other specified nodes was extracted and recorded (see raw values in S1
228 Fig). A Bonferroni correction was used to correct the p -value for multiple comparisons between
229 nodes (p -value of $0.05/7 = 0.00714$). The corrected p -values, representing covariance statistics
230 between nodes (i.e. the seed used in each of the seven MACMs) and projections (i.e. the
231 connectivity from the MACM of seed ROI to the six other ROIs), were used to generate the
232 edges in the meta-analytic connectivity model. Connections between the identified peak regions
233 were mapped as nodes exhibiting one-way, two-way, or no significant connections to each other.
234 If only one edge between two nodes was significant (i.e. a significant connection from MACM
235 of ROI 1 to seed 2), the connection was considered unidirectional. On the other hand, if both
236 edges between two nodes were significant (i.e. a significant connection from MACM of seed 1 to
237 ROI 2 and a significant connection from MACM of seed 2 to ROI 1), the connection was
238 considered bidirectional.

239 **Paradigm class and behavioral domain analyses**

240 Paradigm class and behavioral domain were also analyzed using the resulting nodes from
241 ALE/MACM and the “Paradigm Analysis” and “Behavioral Analysis” plugins for Mango [32].
242 Paradigm class is a category in BrainMap classifying what experimental task was used.
243 Behavioral domain is a BrainMap category classifying the mental operations likely to be isolated
244 by a given contrast. Laird et al. [33] found that these two fields provide the most salient
245 information for ascertaining a brain region’s function. These analyses assume that the spatial
246 distribution of activation foci derived from BrainMap’s database for each behavioral sub-domain
247 or paradigm class represents that sub-domain’s (or class’s) true probability distribution function

248 [32]. Z-scores are generated for observed-minus-expected values for each behavioral sub-domain
 249 or paradigm class. Lancaster et al. [32] state that only z-scores greater than or equal to 3.0 are
 250 significant (comparable to a *p*-value of 0.05 with Bonferroni correction for multiple
 251 comparisons). The identification of paradigm class and behavioral domain associated with nodes
 252 aids interpretation of connectivity reported via MACM.

253 Results

254 ALE results for deceptive versus honest behavior

255 45 studies, 977 foci and 2,836 subjects were included in the ALE meta-analysis to
 256 demonstrate activation associated with deceptive versus honest behavior. The D > H ALE
 257 revealed seven significant clusters (Table 2). The nearest grey matter associated with each cluster
 258 are the left and right insula (L Ins, R Ins), left superior frontal gyrus (L SFG), left and right
 259 supramarginal gyrus (L SMG, R SMG), and left and right medial frontal gyrus (L MFG, R
 260 MFG). Fig 2 depicts activation of each of the 7 clusters.

261 **Table 2. Deceptive > Honest ALE results.**

262

Cluster #	x	y	z	ALE	P	Z	Label (Nearest Gray Matter within 5mm)
1	-34	24	0	0.0623387	2.11E-14	7.5542035	<i>Left Insula (BA 13)</i>
	-34	22	-8	0.05769345	4.72E-13	7.1385703	Left Inferior Frontal Gyrus (BA 47)
	-52	20	-2	0.04107672	1.51E-08	5.539762	Left Inferior Frontal Gyrus
	-52	18	12	0.03158789	3.17E-06	4.5147033	Left Inferior Frontal Gyrus (BA 44)
	-44	8	24	0.02707989	3.36E-05	3.9858272	Left Inferior Frontal Gyrus (BA 9)
	-44	18	22	0.02419243	1.42E-04	3.6286738	Left Middle Frontal Gyrus (BA 9)
2	-2	18	50	0.0674078	6.51E-16	7.994921	<i>Left Superior Frontal Gyrus (BA 6)</i>
	-6	14	56	0.05541562	2.09E-12	6.931297	Left Superior Frontal Gyrus (BA 6)
	8	12	62	0.0395192	3.77E-08	5.3780737	Right Medial Frontal Gyrus (BA 6)
	-6	34	48	0.02794396	2.16E-05	4.0891724	Left Superior Frontal Gyrus (BA 8)
	8	20	38	0.02459265	1.17E-04	3.6790812	Right Cingulate Gyrus (BA 32)

	6	36	40	0.02218968	3.74E-04	3.3712685	Right Medial Frontal Gyrus (BA 8)
3	<i>40</i>	<i>18</i>	<i>-2</i>	<i>0.0584591</i>	<i>2.84E-13</i>	<i>7.208284</i>	<i>Right Insula</i>
	34	24	-4	0.05275477	1.17E-11	6.683431	Right Insula
	52	16	-12	0.03045653	5.80E-06	4.385135	Right Inferior Frontal Gyrus (BA 47)
	50	22	-16	0.02702516	3.45E-05	3.979767	Right Inferior Frontal Gyrus (BA 47)
	56	14	2	0.02278692	2.81E-04	3.4494302	Right Precentral Gyrus (BA 44)
4	<i>50</i>	<i>-46</i>	<i>40</i>	<i>0.0593763</i>	<i>1.54E-13</i>	<i>7.2910028</i>	<i>Right Supramarginal Gyrus (BA 40)</i>
	54	-52	34	0.04975116	7.81E-11	6.3994093	Right Supramarginal Gyrus (BA 40)
	42	-44	38	0.04800459	2.32E-10	6.230713	Right Supramarginal Gyrus (BA 40)
	38	-52	46	0.02770078	2.45E-05	4.0604396	Right Inferior Parietal Lobule (BA 40)
5	<i>-58</i>	<i>-50</i>	<i>32</i>	<i>0.0516142</i>	<i>2.41E-11</i>	<i>6.576254</i>	<i>Left Supramarginal Gyrus (BA 40)</i>
	-44	-46	44	0.04175625	1.01E-08	5.609538	Left Inferior Parietal Lobule (BA 40)
	-50	-52	48	0.03441323	6.81E-07	4.8303714	Left Inferior Parietal Lobule (BA 40)
6	<i>-40</i>	<i>12</i>	<i>46</i>	<i>0.0343478</i>	<i>7.04E-07</i>	<i>4.823757</i>	<i>Left Middle Frontal Gyrus (BA 6)</i>
	-42	18	38	0.03313847	1.37E-06	4.6894875	Left Middle Frontal Gyrus (BA 9)
	-42	-2	50	0.02910901	1.18E-05	4.227779	Left Precentral Gyrus (BA 6)
	-40	26	32	0.02852156	1.60E-05	4.158152	Left Middle Frontal Gyrus (BA 9)
7	<i>48</i>	<i>24</i>	<i>30</i>	<i>0.0368345</i>	<i>1.76E-07</i>	<i>5.09343</i>	<i>Right Middle Frontal Gyrus (BA 9)</i>
	38	30	34	0.02526887	8.36E-05	3.7640233	Right Middle Frontal Gyrus (BA 9)

263 Reported in MNI coordinates with corresponding ALE, P, and Z values. Peak coordinate
 264 information is in italics.

265 **Fig 2. Deceptive > Honest ALE results.** Activation is visualized in Mango on a standard MNI
 266 brain template (**A**: horizontal slice, **B**: coronal slice; FWE < 0.001, p < 0.001, at 5,000
 267 permutations). Z and Y values correspond to the brain slice label. The activation color (red-
 268 yellow) corresponds to the ALE value listed in **Table 2**. Left and right are accurately depicted.

269 **MACM results for deceptive versus honest behavior**

270 MACM was used to examine the extent of connectivity between the seven clusters
 271 identified in the ALE exhibiting greater activation during deception than honest behavior. A
 272 unique MACM was carried out for each individual ROI, resulting with seven independent seed
 273 to voxel connectivity maps. Bolded lines (Figs 3A and B) represent bidirectionality, indicating

274 that the variance in two nodes is predictive of each other. Arrows (Figs 3A and B) represent
275 unidirectionality, indicating that variance in one node is predictive of variance in another, but not
276 vice versa. The matrix results are shown in Fig 3C (raw scores: S1 Fig).

277 Significant one-way functional connectivity is shown projecting from: R SMG to L Ins, L
278 SFG, and from L SMG to L Ins, R Ins, L SFG, L MFG, R MFG. Significant two-way functional
279 connectivity is shown involving: L Ins to L SFG, R Ins, R MFG; L SFG to R Ins, L MFG, R
280 MFG; R Ins to R SMG, R MFG; R SMG to L SMG, L MFG, R MFG.

281 **Fig 3. Meta-analytic model of connectivity between Deceptive > Honest peak regions. A:**
282 horizontal slice and **B:** coronal slice. Data were visualized with the BrainNet Viewer [34]
283 (<http://www.nitrc.org/projects/bnv/>). **Key** (ROI Labels): 1: left insula (L Ins); 2: left superior
284 frontal gyrus (L SFG); 3: right insula (R Ins); 4: right supramarginal gyrus (R SMG); 5: left
285 supramarginal gyrus (L SMG); 6: left medial frontal gyrus (L MFG); 7: right medial frontal
286 gyrus (R MFG). **(C)** The matrix depicting connectivity from seed regions (left column) to the
287 whole brain (“1” dark blue: bidirectional; “1” light blue: unidirectional; “0”: no direction
288 implied).

289 **Paradigm class and behavioral domain results**

290 Using Lancaster et al.’s [32] “Paradigm Class” Mango plugin for analysis of BrainMap’s
291 functional database of healthy subjects, 14 significant paradigm classes were related to the seven
292 nodes identified in the D > H ALE meta-analysis. Fig 4A indicates paradigm classes for which
293 the observed regional number of experiments was higher than expected (compared with the
294 distribution across the BrainMap database). All paradigm classes at a z -score of ≥ 2.0 are
295 reported in S4 Table. The left insula has the strongest association with the paradigm class
296 “Reward” ($z = 4.564$). The left SFG has the strongest association with the paradigm class of

297 “Finger Tapping/Button Press” ($z = 4.905$). The right insula has the highest association with the
298 paradigm class “Pain Monitor/Discrimination” ($z = 5.550$). These paradigm class analysis results
299 indicate significant associations of the left and right insula with reward paradigms, in addition to
300 significant associations of left SFG and right insula to semantic discrimination and pain
301 discrimination, respectively.

302 Subsequent behavioral domain analysis of the seven nodes from ALE/MACM with the
303 “Behavioral Analysis” Mango plugin [32] identified 15 significant sub-domains. Fig 4B
304 indicates behavioral sub-domains (within one of five domains) for which the observed regional
305 number of experiments was higher than expected (compared with the distribution across the
306 BrainMap database). All sub-domains at a z -score of ≥ 2.0 are reported in S5 Table. The left
307 insula has the strongest association with sub-domains of “Cognition”, including “Language
308 (Speech)” ($z = 6.097$), “Language (Semantics)” ($z = 6.037$), “Attention” ($z = 5.837$), and
309 “Reasoning” ($z = 5.693$). The left SFG also has strong associations with sub-domains of
310 “Cognition”, including “Attention” ($z = 6.78$), “Memory (Working)” ($z = 5.829$), and “Language
311 (Semantics)” ($z = 5.335$). The right insula has strongest associations with “Attention” of the
312 “Cognition” domain ($z = 6.421$) and “Somesthesia (Pain)” of the “Perception” domain ($z =$
313 5.417). The right MFG has one significant association with the “Attention” sub-domain of
314 “Cognition” ($z = 3.124$). These results indicate that the bilateral insula, L SFG, and R MFG are
315 mainly associated with behaviors regarding cognition.

316 **Fig 4. Z-scores of (A) paradigm class or (B) behavioral domain analyses.** In the Behavioral
317 Domain panel (B), the Emotion and Interoception domains are abbreviated as “E” and “I”
318 respectively. Only paradigm classes or behavioral sub-domains passing the threshold of $z \geq 3.0$
319 are depicted.

320 **Discussion**

321 In the presented series of meta-analyses, we conducted activation likelihood estimation
322 and meta-analytic connectivity modelling in addition to subsequent paradigm class and
323 behavioral domain analyses using reported neuroimaging findings for deception tasks.

324 **Regions associated with deception**

325 The findings of this study align well with previously reported findings while presenting
326 new information regarding functional connectivity of deception-related brain regions. Results
327 from the ALE identified seven brain regions significantly activated during deception, including
328 bilateral insula, left superior frontal gyrus, bilateral supramarginal gyrus, and bilateral medial
329 frontal gyrus. These regions match regions reported in previous meta-analyses: BA 6 (SFG), BA
330 40 (IPL or SMG), BA 6 (MFG). Our first hypothesis was supported in that the study replicates
331 findings of prefrontal (BA 9 and 13) and memory-related (BA 6) regional activation during
332 deception. Various additional regions were consistently active, most likely resulting from the
333 variety of paradigms included in ALE. Interestingly, the regions that we found to be significantly
334 active during deception tasks matched those reported in the most recent meta-analysis [13]. Here
335 we discuss each region's functional significance, relationship to sociocognitive behaviors of
336 deception, and make comparisons to existing deception literature.

337 **Insula**

338 Recent studies using ecologically valid paradigms involved more of the participants'
339 emotions as evidenced by consistent activation in the insula and other emotion-related brain
340 regions [35]. These recent studies have added evidence that the insula is part of a reflexive,
341 automatic system of social cognition. In Baumgartner et al.'s study [35], results demonstrated

342 increased activation of the anterior insula in dishonest subjects compared to honest subjects.
343 Further, the researchers state that subjects in the dishonest group who later intended to break
344 promises demonstrate increased bilateral frontoinsula cortex activation during that (promise)
345 stage. Proposed reasons for insular activity in dishonesty or deception include insular activation
346 during aversive emotional experiences associated with unfairness, threat of punishment, and
347 anticipation of negative/unknown emotional events [35]. The researchers also state that aversive
348 experiences may include “guilty conscience” towards the other individual who will eventually be
349 misled.

350 **Superior frontal gyrus**

351 The SFG has been associated with cognitive processes such as working memory,
352 response inhibition, task switching, visual attention, and theory of mind [13]. More specific to
353 deception behavior, Chen et al. [36] reported overlapping SFG activation between feigned short-
354 term and long-term memory. This finding supports the role of SFG in executive function aspects
355 of feigned memory impairment, whether short-term or long-term memory [36]. In addition, Yin
356 et al. [37] reported that both spontaneous and instructed lying coactivate the SFG among other
357 regions. Researchers also report the involvement of SFG in identity faking aspects of deception
358 behavior [38]. Since SFG has implications with working memory, Ding et al. [38] state that both
359 SFG and working memory functions play a role in deceptively faking one’s identity.

360 **Supramarginal gyrus**

361 The supramarginal gyrus lies within the inferior parietal lobule, an area commonly
362 associated with deception since the pioneering neuroimaging study by Spence et al. [6].
363 Instructed deception has been shown to involve the IPL [37]. Various other studies have
364 associated the inferior parietal regions with the execution of deception. Ito et al. [39] reported

365 increased SMG activity in the execution phase of a deception task compared with telling the
366 truth. Kireev et al. [40] found a similar result in that a network including the IPL demonstrated
367 increased activation during deliberate deception processing/execution. In addition, Ofen et al.
368 [41] found similar activation of parietal regions during the execution of a deceptive response.
369 Potential reasons for the involvement of SMG/IPL in executing deception include parietal
370 regions supporting executive functioning (i.e. working memory) [39] and cognitive control
371 processes as they are commonly activated during tasks that require high levels of cognitive
372 control [41]. Further evidence of this comes from a study where activation of parietal regions
373 was associated with intentional feigned responses and not unintentional errors [41].

374 It has also been suggested that SMG/IPL is engaged when detecting salient stimuli and
375 processing judgements regarding deception [10] as well as probability monitoring and response
376 counting [5]. Browndyke et al. [5] state that these sociocognitive aspects may allow the deceiver
377 to lie less obviously, or better feign an impairment. Further, the study participants subsequently
378 reported attempts to gauge the proportion of their true versus feigned responses in order to create
379 less detectable deception [5]. Along this line of thought, the parietal regions (SMG/IPL) have
380 been associated with theory of mind [13]. Theory of mind necessitates the ability to understand
381 and predict another individual's behavior (via inferences regarding mental state, intentions,
382 feelings, expectations, beliefs, or knowledge) and to cognitively represent one's own mental state
383 [42]. Evidence of the association between SMG and the sociocognitive process of theory of mind
384 includes the activation of SMG in pro-social lying that was deemed morally appropriate [43] and
385 the recruitment of IPL regions for top-down modulation of emotional responses [44].

386 **Medial frontal gyrus**

387 Frontal (namely prefrontal) regions have markedly been reported in association with
388 deception tasks and behaviors. Sun et al. [45] demonstrated that lies elicited stronger MFG
389 activation compared to truth. Moreover, Bhatt et al. [46] state that MFG may play a role in
390 familiarity-based deception (rather than familiarity or deception individually). Liu et al. [47]
391 stated that (left) MFG seemed to be primarily responsible for the falsification process in
392 conditional proposition testing. The researchers noted the association between MFG and working
393 memory and higher-level control processes (i.e. coordinating widely distributed cognitive and
394 emotional reactions, learning new rules, and processing logical relationships) [47]. Further,
395 involvement of frontal lobe regions is consistent with the conceptualization of deception as an
396 executive control incentive task [11,48].

397 **Connectivity analyses**

398 Our second hypothesis was also supported by the involvement of the prefrontal and
399 memory-related regions in the connectivity model. The connectivity modelling used in the
400 current meta-analysis, which adds new information regarding deception-related brain regions,
401 has not been done in this realm of research before to our knowledge. MACM of brain regions
402 active during deception, identified via ALE, show that these regions are also highly connected to
403 each other. Each of the seven nodes were involved in at least one significant bidirectional
404 connection. Interestingly, only the seed nodes for left and right supramarginal gyri projected to
405 other nodes (in other words, were involved in unidirectional connections). Thus, activation of
406 SMG is likely predictive of activation in bilateral insula, left SFG, or bilateral MFG
407 (respectively). This means that the bilateral SMG must engage with other regions to engage in
408 deception tasks, however those other regions are not required for deception. Other regions
409 identified in our deception ALE (i.e. bilateral insula, left SFG, bilateral MFG) likely have

410 supportive roles in cognitive aspects of the tasks. This may well be the case since, in order to lie,
411 an individual must construct new information while withholding factual information during a
412 social interaction with another individual [49]. The important role SMG plays in deception is
413 further supported by our paradigm class and behavioral domain findings. The bilateral SMG did
414 not elicit significant (z -score ≥ 3.0) paradigm class or behavioral domain information that
415 would indicate SMG involvement in other cognitive/task-based aspects in the current meta-
416 analysis. Together, the connectivity model, paradigm class, and behavioral domain findings of
417 the current study could implicate the supramarginal gyrus as a key region in a brain network that
418 allows individuals to successfully deceive one another.

419 **Importance of neuroimaging deception and its application**

420 A major motivation behind the study of deception is the ability to reliably detect when a
421 given individual is being truthful or is lying [11]. The law often concerns itself with this
422 phenomenon as it contributes to judgements regarding human behavior. Untruthful statements
423 are possible and commonly made by plaintiffs, defendants, and witnesses alike [50]. Assessing
424 the veracity of statements made by individuals inside and outside of the courtroom is a crucial
425 component of just and efficient legal resolution [50]. Legal actors increasingly offer
426 neuroscientific evidence during litigation and policy discussions. Similarly, cognitive
427 neuroscientists aim to address important problems confronted by the law by explaining
428 neuropsychological mechanisms that give rise to thoughts and actions [51]. The utility of
429 neuroscientific evidence depends both on the accuracy of the neuroscience as well as the
430 appropriate usage by legal actors. Though specific courtroom scenarios deal with individuals,
431 group-level studies are needed as fMRI-based evidence will be used to establish the reliability of
432 instances related to any deception apparent in court [50]. Accurate detection of deception in

433 humans is of particular importance in ensuring valid and just forensic practices and legal
434 proceedings.

435 Where the legal system and neuroscience overlap is in the attempts to utilize
436 neuroscientific advances to yield better answers to legally relevant questions that have had
437 historically unsatisfying solutions [51]. Some questions include whether or not an individual is
438 responsible for their behavior, if an individual is competent, what an individual remembers, and
439 pertaining to the current meta-analysis, if an individual is lying. Legal cases from the last decade
440 or so have involved methods of brain-based lie detection, brain-based memory detection
441 (wherein under controlled experimental conditions memory states may be detected using fMRI
442 data), detection and classification of “culpable mental states” including purposeful, knowing,
443 reckless, and negligent (based on the “Model Penal Code”), and investigations of the decision-
444 making processes of, not only if an individual is criminally liable, but also how to then punish
445 that individual in an unbiased and just fashion [51]. However, all of these aspects pertaining to
446 criminal law have their apparent downfalls (for more on this see [51]). Those at the intersection
447 of neuroscience and the law (commonly called “neurolaw”) focus on non-criminal law as well:
448 the aging brain in regard to wills, trusts, and estates; disability and social security laws in
449 association with the neuroscience of pain; similarly, brain injury cases and medical malpractice;
450 and more.

451 Neuroimaging has been used in legal proceedings since the early twentieth century, with
452 use of electroencephalography (EEG) appearing in the 1940s, computed tomography (CT)
453 appearing in 1981, positron emission tomography (PET) appearing in 1992, and fMRI not long
454 after [52]. Over the last two decades alone, the use of neuroscientific evidence in general and
455 neuroimaging-based evidence specifically has increased tremendously in the United States [52].

456 Jones [53] has identified seven categories for the applications of neuroscience to the legal
457 setting: buttressing, detecting, sorting, challenging, intervening, explaining, and predicting. We
458 believe this meta-analytic view of deception fits into the detecting and explaining categories,
459 wherein neuroscience is used to gain otherwise elusive insights and to shed light on not well
460 understood phenomenon. Our work contributes to efforts of detecting deception-based activity in
461 the functional brain rather than the activity of the nervous system (i.e. heart rate/blood pressure,
462 respiration, skin conductivity, etc. used in polygraphy). Benefits of this have been reviewed at
463 length [54]. In agreement with what is written in a recent review [51], we believe that there is a
464 common ground where the long-term effects of neuroscience on law are not overstated but we
465 can appropriately consider that neuroscience has something useful to offer the legal system.

466 **Challenges and limitations**

467 Spence et al. [49] predicted the problems that have persisted in the neuroimaging
468 literature of deception: 1) ecological validity: the experiments generally involve compliant
469 subjects who are not involved in high-stakes situations that pertain to forensics or the legal
470 system (thus, these studies are unable to address how the brain functions when someone is
471 intentionally lying to cause harm or deceive for a known purpose and may not extrapolate to
472 circumstances wherein deception is an automatic process driving malevolent behavior) [40]; 2)
473 experimental design: some experiments have simple designs of simulated deception that
474 facilitate simple contrasts (lie > truth) which may not cohere in the real world (where there exists
475 imprecise information, mixed motives, etc.); 3) statistical power: there may well be a range of
476 individual differences that would make it premature to extrapolate from neuroimaging data to an
477 individual suspect in a courtroom.

478 The current meta-analysis regarding brain regions active during deceptive versus honest
479 behavior addresses the above problems to some degree by including ecologically valid studies in
480 our total pool and drawing results from a large, heterogeneous sample. More recently, studies and
481 their respective paradigms have attempted to evoke “realistic social exchanges” by allowing
482 participants the free choice to break or keep a promise, mitigating to some degree the previous
483 work. These ecologically valid studies were included in our current meta-analyses. Also, the
484 nature of coordinate-based meta-analyses that include task-based studies allows results to be
485 drawn from a large, heterogeneous sample. This takes into account paradigms that may or may
486 not involve compliant subjects in somewhat realistic circumstances, and that may or may not
487 include “simple contrasts”, as long as the inclusion criteria are met. Regarding statistical power,
488 the recommended number of included experiments has been met in the current meta-analysis (20
489 experiments in order to achieve sufficient statistical power) [55].

490 **Future Directions**

491 Due to the previously noted association of supramarginal gyrus and theory of mind
492 aspects of deception, a potential next step could be analyzing regions found in the current study
493 with regions involved in theory of mind. Deception is related to theory of mind, as deceiving
494 another individual necessitates knowledge of the victims’ thoughts and beliefs as well as analysis
495 of responses to the lie made in the social context [11]. Thus, follow-up meta-analyses can be
496 conducted and subsequently compared to the findings of the current study to determine if
497 overlapping regional activation exists. Of particular interest in such a comparison would be the
498 SMG and SFG which have been associated with theory of mind aspects of deception.

499 **Conclusion**

500 The current study utilized activation likelihood estimation and the novel approaches of
501 meta-analytic connectivity analysis, paradigm class analysis, and behavioral domain analysis to
502 investigate neuroanatomical correlates of deception and their functional connectivity. Across the
503 varying studies involving differences in context of deception, motivation for deception, response
504 modality, and more, we found significant activation in the insula, superior and medial frontal
505 gyri, and supramarginal gyrus. Moreover, the connectivity model and paradigm/behavioral
506 analyses demonstrate the key role that the supramarginal gyrus has in the brain network
507 associated with deceptive acts and behaviors. An understanding of the neurobiological aspects of
508 deception has implications for subsequent theory of mind and social cognition research in
509 addition to forensic/legal analyses of guilt and responsibility.

510 **Acknowledgements**

511 We acknowledge and are grateful for the help of Noah Waller, Laura Ireland, Ariana
512 White, and Jenelle Delfino in coding papers for Sleuth, instruction for analyses, and preparing
513 the manuscript. This work is supported by Fund IGF062 Program Neuroscience and Behavioral
514 Health at the University of New Hampshire.

515 **References**

- 516 1. Merriam-Webster.com [Internet]. Deception. Merriam-Webster dictionary. [cited 2021 Jan
517 11]. Available from <https://www.merriam-webster.com/dictionary/deception>
- 518 2. Zuckerman M, Koestner R, Driver R. Beliefs about cues associated with deception. *J*
519 *Nonverbal Behav.* 1981 Dec;6(2):105-114. <https://doi.org/10.1007/BF00987286>.
- 520 3. Abe N. How the brain shapes deception: an integrated review of the literature.
521 *Neuroscientist.* 2011 Oct;17(5):560-74. <https://doi.org/10.1177/1073858410393359>
- 522 4. Hare RD, Neumann CS. Psychopathy as a clinical and empirical construct. *Annu Rec Clin*
523 *Psychol.* 2008;4:217-46. <https://doi.org/10.1146/annurev.clinpsy.3.022806.091452>
- 524 5. Browndyke JN, Paskavitz J, Sweet LH, Cohen RA, Toker KA, Welsh-Bohmer KA, et al.
525 Neuroanatomical correlates of malingered memory impairment: event-related fMRI of
526 deception on recognition memory task. *Brain Inj.* 2008 Jun;22(6):481-9.
527 <https://doi.org/10.1080/02699050802084894>

- 528 6. Spence SA, Farrow TF, Herford AE, Wilkinson ID, Zheng Y, Woodruff PW. Behavioural
529 and functional anatomical correlates of deception in humans. *Neuroreport*. 2001 Sep
530 17;12(13):2849-53. <https://doi.org/10.1097/00001756-200109170-00019>
- 531 7. Langleben DD, Schroeder L, Maldjian JA, Gur RC, McDonald S, Ragland JD, et al. Brain
532 activity during simulated deception: an event-related functional magnetic resonance study.
533 *Neuroimage*. 2002 Mar;15(3):727-32. <https://doi.org/10.1006/nimg.2001.1003>
- 534 8. Lee TMC, Liu HL, Tan LH, Chan CC, Mahankali S, Feng C, et al. Lie detection by
535 functional magnetic resonance imaging. *Hum Brain Mapp*. 2002 Mar;15(3):157-64.
536 <https://doi.org/10.1002/hbm.10020>
- 537 9. Ganis G, Kosslyn SM, Stose S, Thompson WL, Yurgelun-Todd DA. Neural correlates of
538 different types of deception: an fMRI investigation. *Cereb Cortex*. 2003 Aug;13(8):830-6.
539 <https://doi.org/10.1093/cercor/13.8.830>
- 540 10. Cui Q, Vanman EJ, Wei D, Yang W, Jia L, Zhang Q. Detection of deception based on fMRI
541 activation patterns underlying the production of a deceptive response and receiving feedback
542 about the success of the deception after a mock murder crime. *Soc Cogn Affect Neurosci*.
543 2014 Oct;9(10):1472-80. <https://doi.org/10.1093/scan/nst134>
- 544 11. Christ SE, Van Essen DC, Watson JM, Brubaker LE, McDermott KB. The contributions of
545 prefrontal cortex and executive control to deception: evidence from activation likelihood
546 estimate meta-analyses. *Cereb Cortex*. 2009 Jul;19(7):1557-66.
547 <https://doi.org/10.1093/cercor/bhn189>
- 548 12. Lisofsky N, Kazzer P, Heerkeren HR, Prehn. Investigating socio-cognitive processes in
549 deception: a quantitative meta-analysis of neuroimaging studies. *Neuropsychologia*. 2014
550 Aug;61:113-22. <https://doi.org/10.1016/j.neuropsychologia.2014.06.001>
- 551 13. Yu J, Tao Q, Zhang R, Chan CCH, Lee TMC. Can fMRI discriminate between deception and
552 false memory? A meta-analytic comparison between deception and false memory studies.
553 *Neurosci Biobehav Rev*. 2019 Sep;104:43-
554 55. <https://doi.org/10.1016/j.neubiorev.2019.06.027>
- 555 14. Eickhoff SB, Bzdok D, Laird AR, Kurth F, Fox PT. Activation likelihood estimation meta-
556 analysis revisited. *Neuroimage*. 2012 Feb 1;59(3):2349-61.
557 <https://doi.org/10.1016/j.neuroimage.2011.09.017>.
- 558 15. Laird AR, Eickhoff SB, Kurth F, Fox PM, Uecker AM, Turner JA, et al. ALE meta-analysis
559 workflows via the BrainMap database: Progress towards a probabilistic functional brain atlas.
560 *Front Neuroinform*. 2009 Jul 9;3:23. <https://doi.org/10.3389/neuro.11.023.2009>
- 561 16. Laird AR, Fox PM, Price CJ, Glahn DC, Uecker AM, Lancaster JL et al. ALE meta-analysis:
562 controlling the false discovery rate and performing statistical contrasts. *Hum Brain Mapp*.
563 2005 May;25(1):155-64. <https://doi.org/10.1002/hbm.20136>
- 564 17. Turkeltaub PE, Eickhoff SB, Laird AR, Fox M, Wiener M, Fox P. Minimizing within-
565 experiment and within-group effects in Activation Likelihood Estimate meta-analyses. *Hum*
566 *Brain Mapp*. 2012 Jan;33(1):1-13. <https://doi.org/10.1016/j.physbeh.2017.03.040>
- 567 18. Robinson JL, Laird AR, Glahn DC, Lovaglio WR, Fox PT. Meta-analytic connectivity
568 modelling: Delineating the functional connectivity of the human amygdala. *Hum Brain*
569 *Mapp*. 2009 Jan 14;31(2):173-84. <https://doi.org/10.1002/hbm.20854>
- 570 19. Robinson JL, Laird AR, Glahn DC, Blangero J, Sanghera MK, Pessoa L, et al. The functional
571 connectivity of human caudate: an application of meta-analytic connectivity modeling with
572 behavioral filtering. *Neuroimage*. 2012 Mar;60(1):117-
573 29. <https://doi.org/10.1016/j.neuroimage.2011.12.010>

- 574 20. Kotkowski E, Price LR, Fox LR, Vanasse TJ, Fox PT. The hippocampal network model: A
575 transdiagnostic metaconnectomic approach. *Neuroimage Clin*. 2018 Jan 8;18:115-129.
576 <https://doi.org/10.1016/j.nicl.2018.01.002>
- 577 21. Eickhoff SB, Jbabdi S, Caspers S, Laird AR, Fox PT, Zilles K, et al. Anatomical and
578 functional connectivity of cytoarchitectonic areas within the human parietal operculum. *J*
579 *Neurosci*. 2010 May 5;30(18):6409-21. <https://doi.org/10.1523/JNEUROSCI.5664-09.2010>
- 580 22. Moher D, Liberati A, Tetzlaff J, Altman DG, PRISMA Group. Preferred reporting items for
581 systematic reviews and meta-analyses: the PRISMA statement. *PLoS Med*. 2009 Jul
582 21;6(7):e1000097. <https://doi.org/10.1371/journal.pmed1000097>
- 583 23. Eickhoff SB, Laird AR, Grefkes C, Wang LE, Zilles K, Fox PT. Coordinate-based activation
584 likelihood estimation meta-analysis of neuroimaging data: A random-effects approach based
585 on empirical estimates of spatial uncertainty. *Hum Brain Mapp*. 2009 Jan;30(9):2907-26.
586 <https://doi.org/10.1002/hbm.20718>
- 587 24. Fox PT, Lancaster JL. Mapping context and content: the BrainMap model. *Nat Rev*
588 *Neurosci*. 2002 Apr;3(4):319-21. <https://doi.org/10.1038/nrn789>
- 589 25. Laird AR, Eickhoff SB, Fox PM, Uecker AM, Ray KL, Saenz JJ. The BrainMap strategy for
590 standardization, sharing, and meta-analysis of neuroimaging data. *BMC Res Notes*. 2011 Sep
591 9;4:349. <https://doi.org/10.1186/1756-0500-4-349>
- 592 26. Fox PT, Laird AR, Fox SP, Fox PM, Uecker AM, Crank M, et al. BrainMap taxonomy of
593 experimental design: description and evaluation. *Hum Brain Mapp*. 2005 May;25(1):185-98.
594 <https://doi.org/10.1002/hbm.20141>
- 595 27. Vanasse TJ, Fox PM, Barron DS, Robertson M, Eickhoff SB, Lancaster JL, et al. BrainMap
596 VBM: an environment for structural meta-analysis. *Hum Brain Mapp*. 2018 Aug;39(8):3308-
597 3325. <https://doi.org/10.1002/hbm.24078>
- 598 28. Langer R, Rottschy C, Laird AR, Fox PT, Eickhoff SB. Meta-analytic connectivity modeling
599 revisited: controlling for activation base rates. *Neuroimage*. 2014 Oct 1;99:559-70.
600 <https://doi.org/10.1016/j.neuroimage.2014.06.007>
- 601 29. Bressler SL, Menon V. Large-scale brain networks in cognition: emerging methods and
602 principles. *Trends Cogn Sci*. 2010 Jun;14(6):277-90.
603 <https://doi.org/10.1016/j.tics.2010.04.004>
- 604 30. Laird AR, Eickhoff SB, Karl L, Robin DA, Glahn DC, Fox PT. Investigating the functional
605 heterogeneity of the default mode network using coordinate-based-meta-analytic modeling. *J*
606 *Neurosci*. 2009 Nov 18;29(46):14496-505. [https://doi.org/10.1523/JNEUROSCI.4004-](https://doi.org/10.1523/JNEUROSCI.4004-09.2009)
607 [09.2009](https://doi.org/10.1523/JNEUROSCI.4004-09.2009)
- 608 31. Smith SM, Fox PT, Miller KL, Glahn DC, Fox PM, Mackay CE, et al. The functional
609 architecture of the human brain: correspondence between resting fMRI and task-activation
610 studies. *Proc Natl Acad Sci U S A*. 2009 Aug 4;106(31):13040-45.
611 <https://doi.org/10.1073/pnas.0905267106>
- 612 32. Lancaster JL, Laird AR, Eickhoff SB, Martinez MJ, Fox PM, Fox PT. Automated regional
613 behavioral analysis for human brain images. *Front Neuroinform*. 2012 Aug 28;6:23.
614 <https://doi.org/10.3389/fninf.2012.00023>
- 615 33. Laird AR, Fox PM, Eickhoff SB, Turner JA, Ray KL, McKay DR, et al. Behavioral
616 interpretations of intrinsic connectivity networks. *J Cogn Neurosci*. 2011 Dec;23(12):4022-
617 37. https://doi.org/10.1162/jocn_a_00077

- 618 34. Xia M, Wang J, He Y. BrainNet Viewer: a network visualization tool for human brain
619 connectomics. PLoS One. 2013 Jul
620 4;8(7):e68910. <https://doi.org/10.1371/journal.pone.0068910>
- 621 35. Baumgartner T, Fischbacher U, Feirabend A, Lutz K, Fehr R. The neural circuitry of a broken
622 promise. Neuron. 2009 Dec 10;64(5):756-70. <https://doi.org/10.1016/j.neuron.2009.11.017>
- 623 36. Chen Z-X, Xue L, Liang X-Y, Mei W, Zhang Q, Zhao H. Specific marker of feigned
624 memory impairment: The activation of left superior frontal gyrus. J Forensic Leg Med. 2015
625 Nov;36:164-71. <https://doi.org/10.1016/j.jflm.2015.09.008>
- 626 37. Yin L, Reuter M, Weber B. Let the man choose what to do: Neural correlates of spontaneous
627 lying and truth-telling. Brain Cogn. 2016 Feb;102:13-25.
628 <https://doi.org/10.1016/j.bandc.2015.11.007>
- 629 38. Ding XP, Du X, Lei D, Hu CS, Fu G, Chen G. The neural correlates of identity faking and
630 concealment: an fMRI study. PLoS One.
631 2012;7(11):e48639. <https://doi.org/10.1371/journal.pone.0048639>
- 632 39. Ito A, Abe N, Fujii T, Hayashi A, Ueno A, Mugikura A, et al. The contribution of the
633 dorsolateral prefrontal cortex to the preparation for deception and truth-telling. Brain Res.
634 2012 Jun 29;1464:43-52. <https://doi.org/10.1016/j.brainres.2012.05.004>
- 635 40. Kireev M, Korotkov A, Medvedeva N, Medvedev S. Possible role of an error detection
636 mechanism in brain processing of deception: PET-fMRI study. Int J Psychophysiol. 2013
637 Dec;90(3):291-9. <https://doi.org/10.1016/j.ijpsycho.2013.09.005>
- 638 41. Ofen N, Whitfield-Gabrieli S, Chai XJ, Schwarlose RF, Gabrieli JDE. Neural correlates of
639 deception: lying about past event and personal beliefs. Soc Cogn Affect Neurosci. 2017 Jan
640 1;12(1):116-127. <https://doi.org/10.1093/scan/nsw151>
- 641 42. Lissek S, Peters S, Fuchs N, Witthaus H, Nicolas V, Tegenthoff M, et al. Cooperation and
642 deception recruit different subsets of the theory-of-mind network. PLoS One. 2008 Apr
643 23;3(4):e2023. <https://doi.org/10.1371/journal.pone.0002023>
- 644 43. Hayashi A, Abe N, Fujii T, Ito A, Ueno A, Koseki Y, et al. Dissociable neural systems for
645 moral judgment of anti-and pro-social lying. Brain Res. 2014 Mar 27;1556:46- 56.
646 <https://doi.org/10.1016/j.brainres.2014.02.011>
- 647 44. Lee TMC, Lee TMY, Raine A, Chan CCH. Lying about the valence of affective pictures: an
648 fMRI study. PLoS One. 2010 Aug
649 25;5(8):e12291. <https://doi.org/10.1371/journal.pone.0012291>
- 650 45. Sun D, Lee TMC, Chan CCH. Unfolding the spatial and temporal neural processing of lying
651 about face familiarity. Cereb Cortex. 2015 Apr;25(4):927-
652 36. <https://doi.org/10.1093/cercor/bht284>
- 653 46. Bhatt S, Mbwana J, Adeyemi A, Sawyer A, Hailu A, VanMeter J. Lying about facial
654 recognition: an fMRI study. Brain Cogn. 2009. Mar;69(2):382-90.
655 <https://doi.org/10.1016/j.bandc.2008.08.033>
- 656 47. Liu J, Zhang M, Jou J, Wu X, Li W, Qiu J. Neural bases of falsification in conditional
657 proposition testing: evidence from an fMRI study. Int J Psychophysiol. 2012 Aug;85(2):249-
658 56. <https://doi.org/10.1016/j.ijpsycho.2012.02.011>
- 659 48. Miyake A, Friedman NP, Emerson MJ, Witzki AH, Howerter A, Wager TD. The unity and
660 diversity of executive functions and their contributions to complex “Frontal Lobe” tasks: a
661 latent variable analysis. Cogn Psychol. 2000 Aug;41(1):49-
662 100. <https://doi.org/10.1006/cogp.1999.0734>

- 663 49. Spence SA, Hunter MD, Farrow TFD, Green RD, Leung DH, Hughes CJ, et al. A cognitive
664 neurobiological account of deception evidence from functional neuroimaging. *Philos Trans R*
665 *Soc Lond B Biol Sci*. 2004 Nov 29;359(1451):1755-62.
666 <https://doi.org/10.1098/rstb.2004.1555>
- 667 50. Adelsheim C. Functional magnetic resonance detection of deception: Great as fundamental
668 research, inadequate as substantive evidence. *Mercer Law Rev*. 2011;62(3):6.
- 669 51. Jones OD, Wagner AD. Law and neuroscience: Progress, promise, and pitfalls. In: Gazzaniga
670 MS, Mangum GR, D Poeppel, editors. *The cognitive neurosciences*. 6th ed. The MIT Press;
671 2018.
- 672 52. Aono D, Yaffe G, Kober H. Neuroscientific evidence in the courtroom: a review. *Cogn*.
673 *Research*. 2019;4(40). <https://doi.org/10.1186/s41235-019-0179-y>
- 674 53. Jones OD. Seven ways neuroscience aids law. In Battro AM, Dehaene S, Sorondo MS,
675 Singer WJ, editors. *Neurosciences and the human person: new perspectives on human*
676 *activities*. Vatican City: The Pontifical Academy of Sciences; 2013. p. 181-194.
- 677 54. Farah MJ, Hutchinson JB, Phelps EA, Wagner AD. Functional MRI-based lie detection:
678 scientific and societal challenges. *Nat Rev Neurosci*. 2014 Feb;15(2):123-31.
679 <https://doi.org/10.1038/nrn3665>
- 680 55. Eickhoff SB, Nichols TE, Laird AR, Hoffstaedter F, Amunts K, Fox PT, et al. Behavior,
681 sensitivity, and power of activation likelihood estimation characterized by massive empirical
682 simulation. *Neuroimage*. 2016 Aug 15;137:70-85.
683 <http://dx.doi.org/10.1016/j.neuroimage.2016.04.072>

684
685 **S1 Fig. Raw values.** The uncorrected estimate of meta-analytic connectivity between each seed
686 region and all other specified nodes.

687
688 **S1 Table. Contrasts included in ALE of all contrasts (D > H, H > D, etc.).** This ALE
689 consisted of 46 studies and 202 experiments with 1,423 foci from 4,678 participants.

690
691 **S2 Table. Results from ALE of all contrasts.** Contrasts included Deceptive > Honest, Honest >
692 Deceptive, etc.

693
694 **S3 Table. Functional MACM workspace information for each node.**

695
696 **S4 Table. Paradigm class analysis results.** Using “Paradigm Analysis” plugin for Mango [32].
697 Z-scores that are significant according to Lancaster et al. [32], meaning they have a z-score of >=
698 3.0, are in bold. However, all z-scores >= 2.0 are reported here.

699
700 **S5 Table. Behavioral domain analysis results.** Using “Behavioral Analysis” plugin for Mango
701 [32]. Z-scores that are significant according to Lancaster et al. [32], meaning they have a z-score
702 of >= 3.0, are in bold. However, all z-scores >= 2.0 are reported here.

703
704 **S6 Table. PRISMA Checklist.**

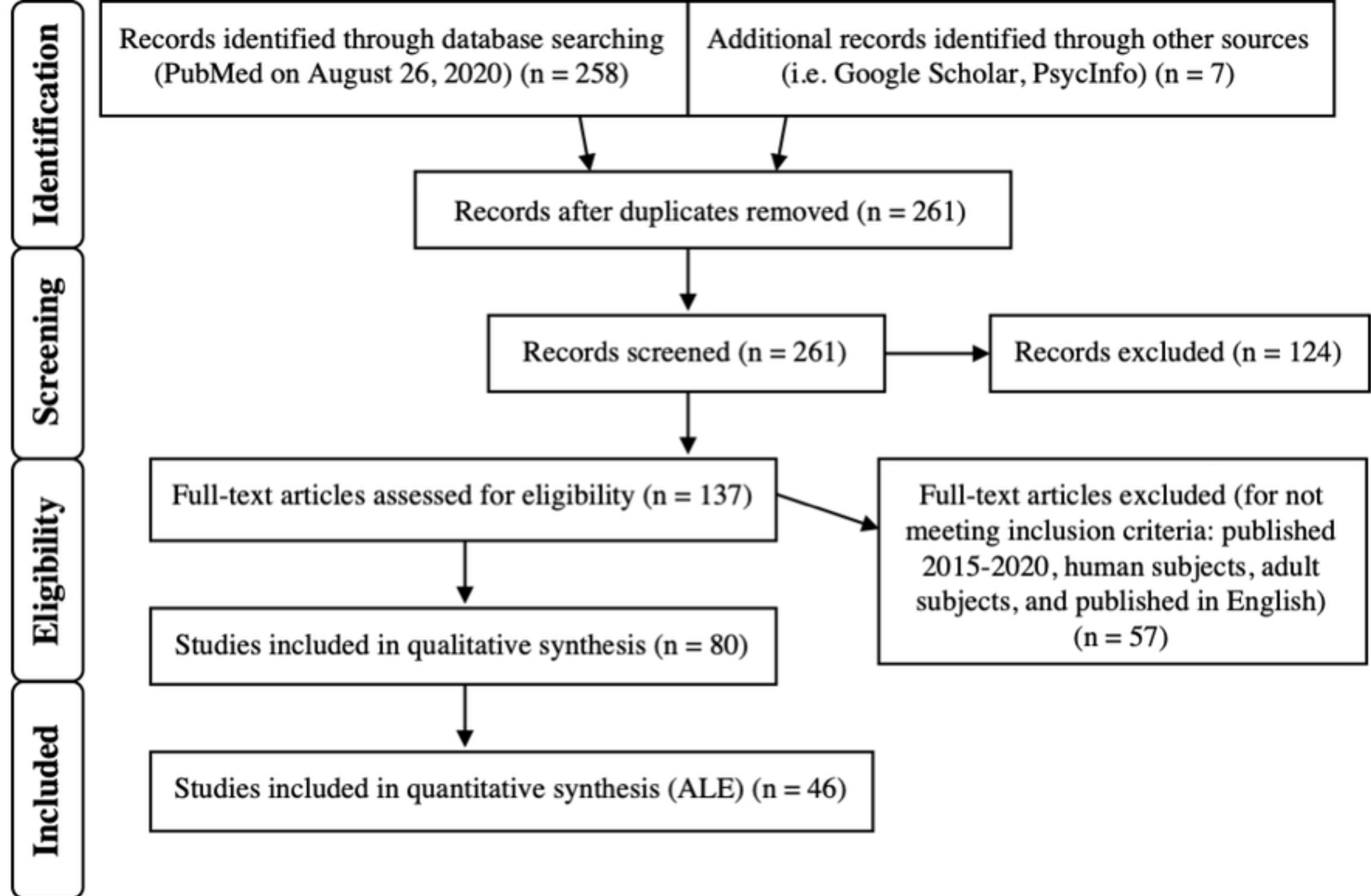


Figure 1

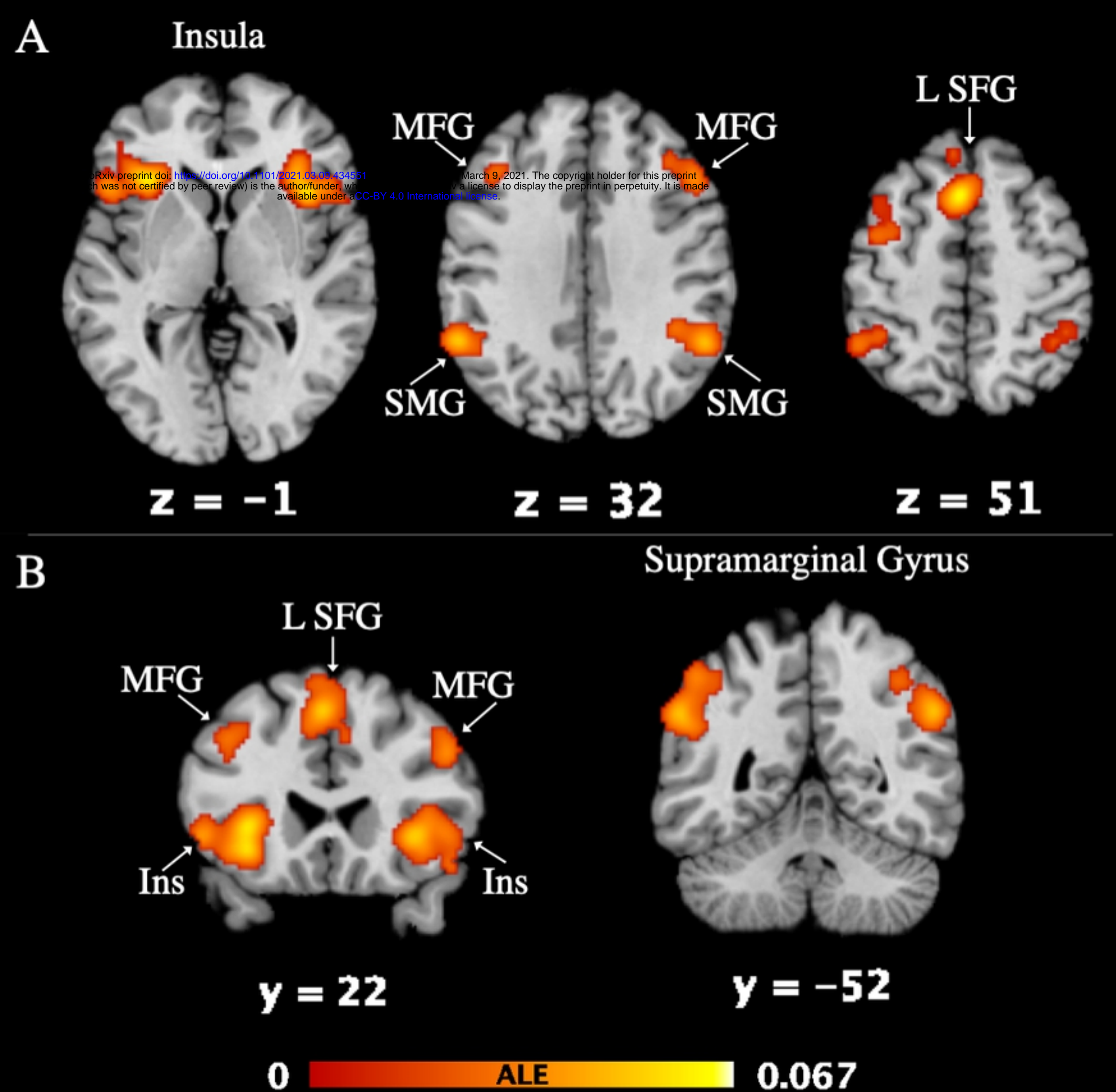
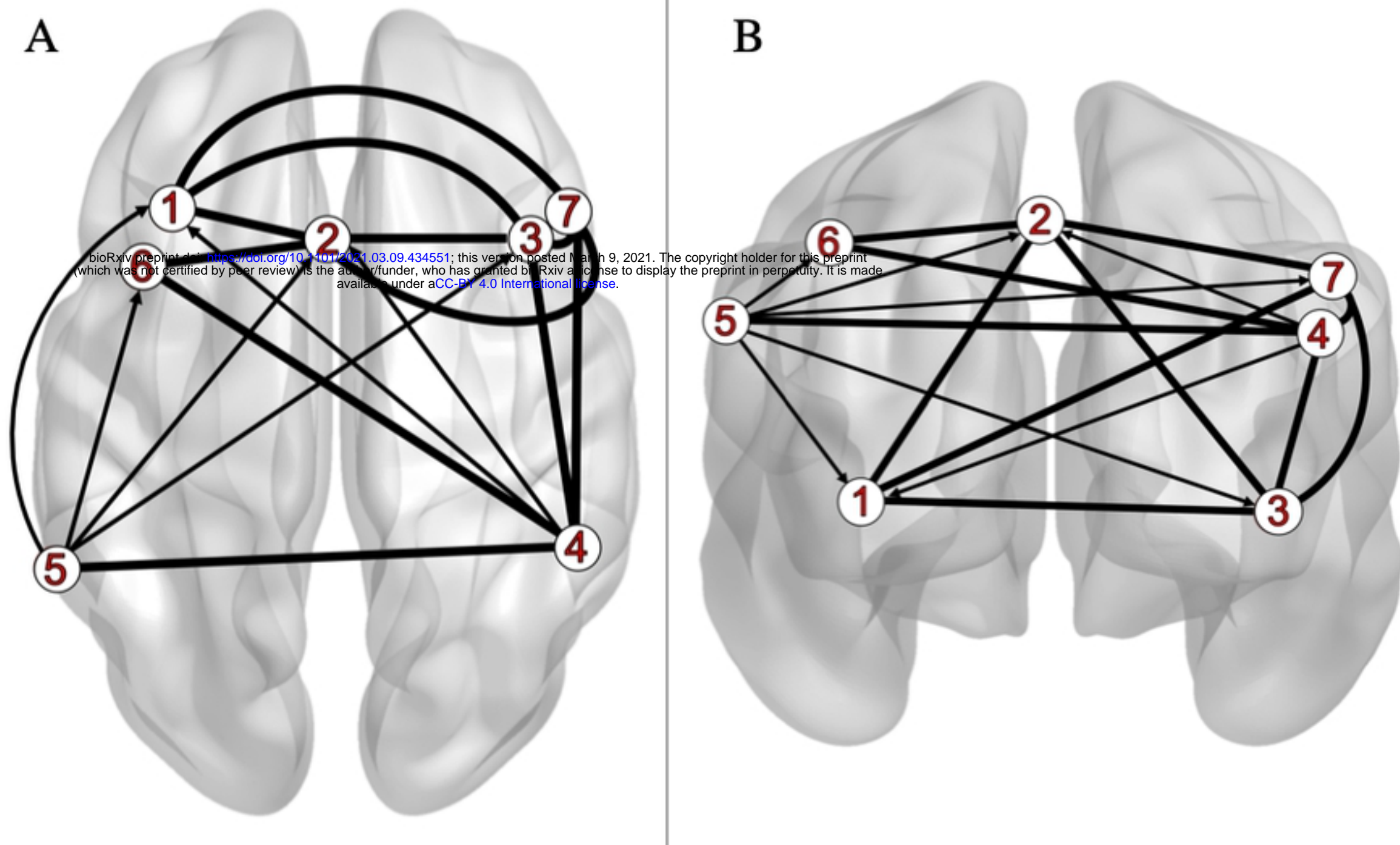


Figure 2



C

	L Ins	L SFG	R Ins	R SMG	L SMG	L MFG	R MFG
L Ins		1	1	0	0	0	1
L SFG	1		1	0	0	1	1
R Ins	1	1		1	0	0	1
R SMG	1	1	1		1	1	1
L SMG	1	1	1	1		1	1
L MFG	0	1	0	1	0		0
R MFG	1	1	1	1	0	0	

Figure 3

A Paradigm Class

B Behavioral Domain

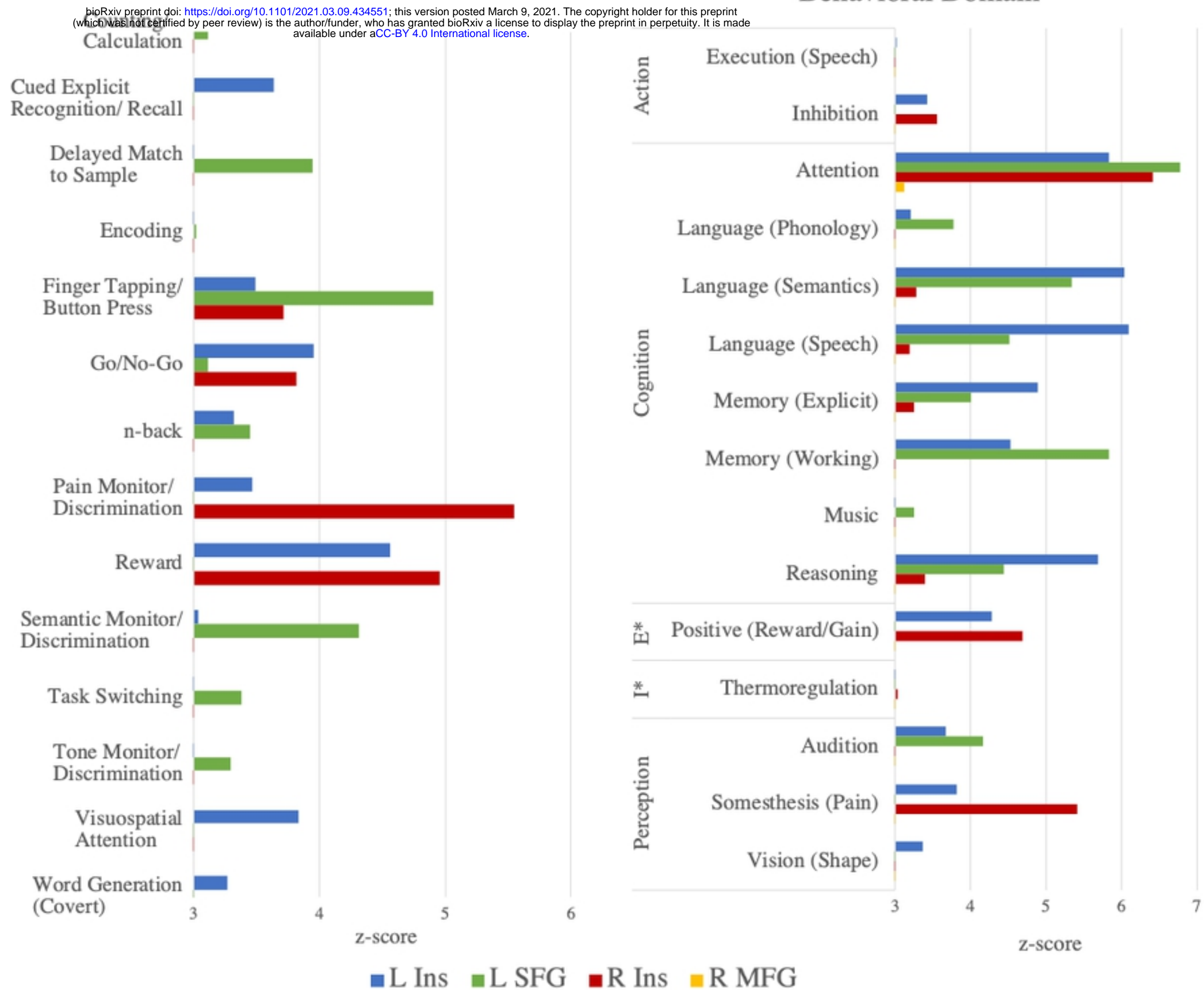


Figure 4